Journal of Power Sources 189 (2009) 1044–1050

Contents lists available at ScienceDirect

Journal of Power Sources

journal homepage: www.elsevier.com/locate/jpowsour

Life prediction of coated and uncoated metallic interconnect for solid oxide fuel cell applications

W.N. Liu*, X. Sun, E. Stephens, M.A. Khaleel

Pacific Northwest National Laboratory, P.O. Box 999, 906 Battelle Boulevard, Richland, WA 99354, United States

ARTICLE INFO

Article history:
Received 16 December 2008
Accepted 29 December 2008
Available online 17 January 2009

Keywords:
Ferritic stainless steel interconnect
Crofer 22 APU
Solid oxide fuel cell (SOFC)
Oxide scale
Spinel coating
Indentation test

ABSTRACT

In this paper, we present an integrated experimental and modeling methodology in predicting the life of coated and uncoated metallic interconnect (IC) for solid oxide fuel cell (SOFC) applications. The ultimate goal is to provide cell designer and manufacture with a predictive methodology such that the life of the IC system can be managed and optimized through different coating thickness to meet the overall cell designed life. Crofer 22 APU is used as the example IC material system. The life of coated and uncoated Crofer 22 APU under isothermal cooling was predicted by comparing the predicted interfacial strength and the interfacial stresses induced by the cooling process from the operating temperature to room temperature, together with the measured oxide scale growth kinetics. It was found that the interfacial strength between the oxide scale and the Crofer 22 APU substrate decreases with the growth of the oxide scale, and that the interfacial strength for the oxide scale/spinel coating interface is much higher than that of the oxide scale/Crofer 22 APU substrate interface. As expected, the predicted life of the coated Crofer 22 APU is significantly longer than that of the uncoated Crofer 22 APU.

1. Introduction

In the recent developments of planar solid oxide fuel cells (SOFCs), several types of ferritic stainless steels have been examined as potential candidates for cell interconnects (ICs) because of their gas-tightness, low electrical resistivity, ease of fabrication, and cost-effectiveness [1]. Compared to chromium-based alloys, iron-based alloys have advantages in terms of high ductility, good workability, and low cost. Iron-based alloys, especially Cr–Fe-based alloys, e.g., Crofer 22 APU and SS441, are the most attractive metallic IC materials for SOFCs [2,3].

Under the typical SOFC operating condition, an oxide layer inevitably forms on the surface of ferritic stainless steels. The oxide scale, consisting mainly of Cr_2O_3, is reported to have relatively good electrical conductivity under the SOFC operating environment. In addition, it protects the alloy substrate from further oxidation. While the formation of this conductive oxide layer is unavoidable, it limits the useful life of these interconnect components if it grows too thick. First of all, the stack electrical resistance will increase with increasing oxide thickness over time. Secondly, under thermal cycling or cooling down to room temperature, the thick oxide scale is prone to spallation because of the mismatch of the coefficient of thermal expansion (CTE) between the oxide scale and the metallic substrate [4]. Many efforts have been undertaken to alleviate or reduce the aforementioned disadvantages of using a Cr-contained alloy for interconnect materials [5–15]. For example, Hua et al. [13] applied relatively dense and well adherent Mn–Co (MC) spinel protection coating with a nominal composition of $MnCo_2O_4$ onto the surfaces of ferritic stainless steel 430 using a sol–gel process. It is demonstrated that the MC spinel protection layer has excellent structural and thermo-mechanical stability, and effectively performs as a mass barrier to the outward diffusion of Cr cations. Yang et al. [15] verified that $(Mn,Co)_3O_4$ spinel demonstrates excellent electrical conductivity, satisfactory thermal and structural stability, and a good thermal-expansion match to ferritic stainless steel interconnects. They pointed out that thermally grown layers of $Mn_{1.5}Co_{1.5}O_4$ not only significantly decreased the contact resistance between the LSF cathode and the interconnect, but also acted as a mass barrier to inhibit scale growth on the stainless steel and to prevent Cr outward migration through the coating.

Even though various coating techniques have shown great potential in slowing down the oxide growth kinetics and in protecting the ferritic stainless steel interconnect under SOFC operating conditions, sub-coating oxide scale growth is still inevitable [16–18]. The appearance and growth of the sub-coating oxide scale will cause growth stress in the oxide scale [19–23]. In addition, the coefficient of thermal-expansion mismatch between the oxide scale and the metallic substrate creates stresses in the scale and on the scale/substrate interface during cooling [23–26]. The growth

* Corresponding author. Tel.: +1 509 372 4967; fax: +1 509 3724672.
E-mail address: wenning.liu@pnl.gov (W.N. Liu).

0378-7753/$ – see front matter © 2009 Elsevier B.V. All rights reserved.
doi:10.1016/j.jpowsour.2008.12.143

stresses in the oxide scale and on the scale/substrate interface combined with the thermal stresses induced by the CTE mismatch between the oxide scale and the substrate may lead to scale delamination/buckling and eventual spallation during stack cooling, which can lead to serious cell performance degradation [26,27]. It is therefore crucial for the cell designers and manufactures to be able to predict and manage the life of the metallic ICs such that it can meet the required design life of the entire SOFC stack. Even though various techniques and methods have been developed to quantify the interfacial strength and fracture toughness between the oxide layer and the metallic substrate [28,29]. IC life prediction methodologies remain to be very scarce in the open literature.

In this paper, we present an integrated experimental/modeling methodology to predict the life of coated and uncoated metallic interconnects. The interfacial strength for the oxide scale/substrate interface and the oxide scale/coating interface are determined by stair-stepping experiments and the corresponding finite element analyses. The critical oxide layer thickness at which delamination will occur upon cooling is determined by comparing the interfacial strength and the cooling-induced interfacial stresses at different interfaces. The life of the metallic interconnect is then quantified by finding the time corresponding to the critical oxide layer thickness on the scale growth kinetics charts. Examples on coated and uncoated Crofer 22 APU are used to demonstrate the analysis procedures. It was found that for Crofer 22 APU, the adhesion strength of the oxide scale/spinel coating interface is much higher than that of the oxide scale/substrate interface, and that cooling-induced delamination occurs on the oxide/substrate interface. The predicted life of the spinel-coated Crofer 22 with 15 μm spinel coating is around 15,500 h, and the predicted life of the uncoated Crofer 22 is only around 4750 h.

2. Stair-stepping indentation experiments

Stair-stepping indentation tests have been used by Sun et al. [30] in quantifying the interfacial strength between the oxide scale and metallic substrate for uncoated Crofer 22 APU. A hardness tester was used to apply the load utilizing a Rockwell diameter ball indenter to the oxide scale on the substrates. The loads were stair-stepped to determine the critical level that spallation occurred on each specimen. In this study, we used the similar experimental procedure on spinel-coated Crofer 22 APU, the goal is to determine the interfacial strength between the spinel coating and the oxide layer.

Fig. 1 shows the SEM image of a typical cross-section of the Crofer/scale/coating tri-layer system. All the specimens were oxidized in air at 800 °C. Metallography was performed to determine the average oxide scale thickness and the spinel coating thickness for each specimen. A hardness tester was used in applying the indentation load on the coating side of the tri-layer system with a Rockwell 1/16 in. diameter ball indenter. The loads were stair-stepped between 60 kgf and 150 kgf to determine the critical load level that spallation occurred on each specimen. When delamination and spallation were observed, the load was typically reduced and the indentation repeated, continually increasing the load with each indent until failure was observed again.

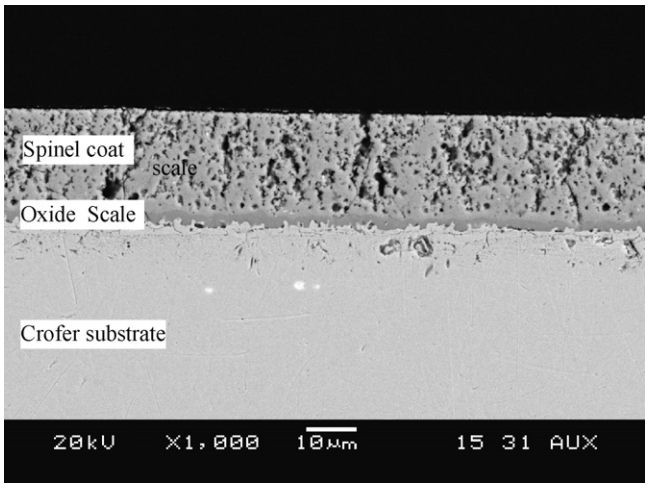

Fig. 1. Scanning electron microscopy (SEM) image of cross-section of Crofer/scale/MC spinel tri-layer system: 600 h oxidized specimen with a measured scale thickness of 1.85 μm and a coating thickness of 19.90 μm.

There are two interfaces in the Crofer/scale/coating system, i.e., the Crofer/scale interface and the scale/coating interface. The indentation-induced delamination may occur on either interface depending on the loading and the corresponding strength of each interface. For each spalled specimen, metallurgical cross-section examination is performed with scanning electron microscopy (SEM) to determine the actual interface at which delamination occurred. Fig. 2 shows the SEM image of a typical cross-section of the Crofer/scale/coating system after spallation was observed during the indentation test. It is clear that the delamination occurs in the interface of the scale and MC spinel coating.

Table 1 lists the indentation test results for two spinel-coated Crofer specimens with different subscale oxide and spinel coating thicknesses. For each specimen, the numbers of indents that either spalled or did not spall are tabulated at each loading level.

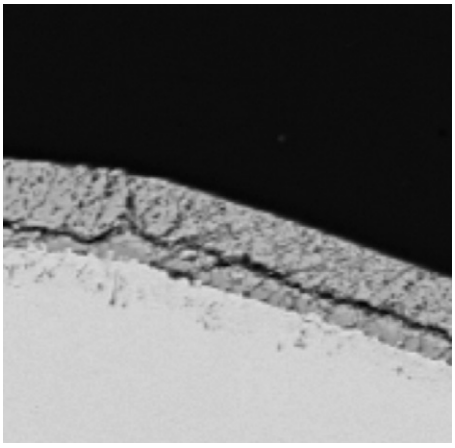

Fig. 2. Typical SEM image of cross-section of Crofer/scale/MC coating system after indentation test: delamination in the scale/MC coating interface.

Table 1
Indentation test results for spinel-coated Crofer with oxide scale.

Spec #	Thickness (μm)		Load (kgf)													
	Scale	Coat	60		75		90		100		115		130		150	
			No spall	Spall	No spall	Spall	No spall	Spall	No spall	Spall	No spall	Spall	No spall	Spall	No spall	Spall
1	1.50	12.93	7	0	4	**3**	3	4	0	7	0	7	0	7	0	7
2	1.85	19.80	3	0	2	0	5	**5**	3	5	0	5	–	–	–	–

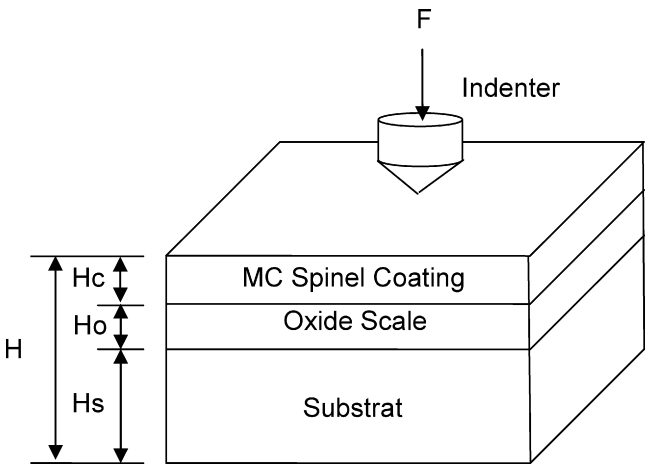

Fig. 3. Schematic of indentation test (no scale).

Generally speaking, the indentation results are quite consistent: at the lowest indentation load of 60 kgf, no spallation was observed for both samples. As the indentation load increases, the number of spalled samples increases and the number of non-spalled samples decreases. Above some critical loads, all the samples experience spallation during indentation. In the indentation test, the load step is 15 kgf due to the limitation of the hardness tester used here. The critical spalling cases are underlined in Table 1 for the two specimens examined.

3. Determination of interfacial shear strength of oxide/spinel coating

In elastic fracture mechanics, the stress intensity factor K is often used to describe the mathematical stress singularity at the tip of the crack in the interfaces. The stress intensity factor can be quantified separately as K_I corresponding to the opening mode; K_{II} corresponding to the in-plane shear mode; and K_{III} corresponding to the out-of-plane tearing mode. Sun et al. [30] reported that for oxidized, uncoated Crofer 22, the interfacial crack tips experience much higher K_{II} than K_I during indentation. Therefore, the interfacial crack growth is considered mostly Mode II dominant during indentation tests, and the interfacial strength is computed through corresponding finite element analysis as the maximum shear stress at the interface induced by the critical indentation force. Similar methodology is adopted in this study for the oxidized, MC spinel-coated Crofer 22. The shear stresses at the interfaces of Crofer/scale and scale/spinel coating are considered as the driving force for the crack propagation at these interfaces.

3.1. Finite element model and material properties

Fig. 3 illustrates the schematic of the indentation test. Taking advantage of the symmetrical nature of the indentation test, two dimensional axisymmetric model is used for maximizing computational efficiency. Commercial finite element (FE) package, ABAQUS [31], is used in simulating the static indentation tests. Fig. 4 shows the typical FE model used, consisting of 124,000 four-node axisymmetric elements with 125,631 nodes. The thickness of the Crofer 22 APU substrate is 0.5 mm. The thicknesses of the oxide scale and the spinel coating are assumed to be uniform in the FE models. Two interfaces are included in this model: one for the oxide scale/substrate and one for the spinel coating/oxide scale. Very fine mesh was used within the indenter contact zone and near the interfaces between the substrate/scale and scale/coating to quantify accurate stress predictions at these locations. The characteristic mesh size at the location for maximum shear stress is around 0.5 μm.

In the early stages of oxidation, the scale exhibited a rough surface and consisted of angular spinel crystals embedded in a chromia substrate. As the time increased to 300 h, the scale surface became smoother as the sharp edges of the spinel phase tended to disappear and the scale began to homogenize. The scale composition and microstructure tended to become homogeneous. After 900 h, the scale surface was even smoother, and the angular spinel crystals had almost totally disappeared, evolving into a fine, agglomerated microstructure [3]. The main composition of the oxide scale for Crofer 22 is Cr_2O_3 and $(Mn,Cr)_3O_4$. The physical and mechanical properties for the oxide scale are taken as $\nu = 0.27$ and $E = 250$ GPa [32,33]. The coefficient of thermal expansion of the oxide scale is 5.7E−6 [32]. The main composition of the MC spinel coating is $Mn_{1.5}Co_{1.5}O_4$; its modulus and Poisson's ratio are measured as $\nu = 0.36$ and $E = 124.7$ GPa, and the coefficient of thermal expansion is measured as 11.5E−6 [34]. Both the oxide scale and the spinel coating are considered as brittle ceramic materials and are modeled as linear elastic materials at room temperature in the indentation analyses. The Crofer 22 APU substrate is considered to be elasto-plastic, based on the properties from ThyssenKrupp [35–37]. This is also evident from the permanent deformation on the indented samples.

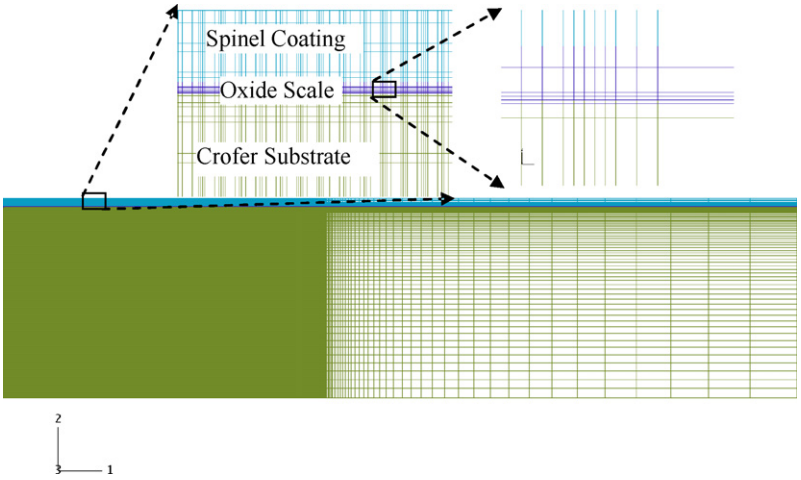

Fig. 4. FE mesh used for Crofer/scale/coating tri-layer system.

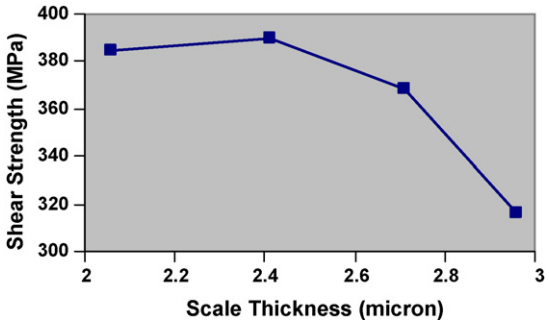

Fig. 5. Predicted interfacial shear strength of oxide/Crofer 22.

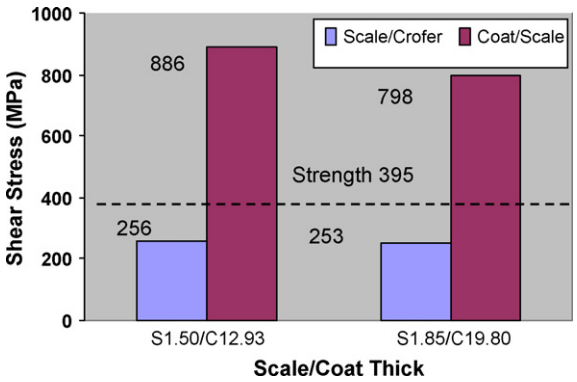

Fig. 6. Modeled maximum interfacial shear stress on different interfaces at critical indentation loads for oxidized spinel-coated Crofer tri-layer systems, where S and C refer to thickness of oxide scale and spinel-coating, respectively.

3.2. Interfacial strength of oxide/Crofer 22 substrate

The interfacial shear strength for the interface of the oxide-scale/substrate for uncoated Crofer 22 was first reported by Sun et al. [30]. In that modeling study, the characteristic mesh size used for the scale/substrate interface is 3 μm and no mesh-size convergence study was reported. Compared to the average oxide scale thickness of 2–5 μm, the mesh size used was relatively coarse. This is particularly true around the turning corner of the oxide scale right underneath the contact radius of the indenter. In this study, a much finer mesh at the interfaces is used, and the characteristic mesh size is 0.5 μm. The same characteristic mesh size is also used for the tri-layer indentation and cooling analyses to minimize the effect of mesh size sensitivity in the tri-layer life predictions. The predicted interfacial shear strength with the current fine mesh is shown in Fig. 5 for various scale thickness.

Results in Fig. 5 indicate that the predicted interfacial strength decreases with increasing scale thickness, i.e., oxide growth. It therefore indicates a degradation of interfacial strength with increasing oxide scale thickness, which in turn suggests a degradation of interfacial strength with increasing exposure and oxidation time. In general, the interfacial strength is considered as an intrinsic property as long as the material system is selected. It should not vary with the thickness of the oxide scale or coating, provided the thickness does not change the characteristic of the interface. The interfacial strength degradation observed here implies that the growth of the oxide scale either changes the interfacial characteristics or alters the chemical composition because of the diffusion of the chromium. A similar phenomenon was reported by Chandra-Ambhorn et al. [38] when they measured the adhesion energy of the thermally grown oxide scale using a room-temperature tensile test to induce spallation. Similar decrease of adhesion energy was reported with increasing oxide thickness.

3.3. Interface strength of spinel-coating/oxide for the tri-layer systems

It is assumed in this study that the interfacial strength for the oxide/Crofer 22 interface is not influenced by the MC spinel coating. The shear strength of this interface therefore stays the same for the uncoated bi-layer Crofer/scale system and spinel-coated tri-layer (Crofer/scale/coating) system. The interfacial strength of oxide/Crofer 22 interface reported in the previous section will be used in the coated tri-layer simulation. FE simulations are performed for the critical indentation cases listed in Table 1 on the spinel-coating/oxide/Crofer tri-layer systems to determine the interfacial strength of oxide scale/spinel coating, see typical FE mesh used in Fig. 4.

The predicted maximum interfacial shear stresses for the two interfaces at the critical indentation loads are shown in Fig. 6 for the two samples. The predicted interfacial shear stresses between the oxide scale and Crofer substrate for the two cases are 253 MPa and 256 MPa, respectively. Both of them are much lower than the oxide scale/Crofer interfacial strength of 395 MPa, as determined in the previous section. Indentation failure is therefore not predicted to occur at this interface. A detailed SEM image of the cross-section of the spinel-coated Crofer after the indentation test shown in Fig. 7 confirm this prediction, i.e., the Crofer 22 and scale interface does not delaminate.

In contrast with the low interfacial shear stresses between the oxide scale and the Crofer 22 APU substrate during indentation, the interfacial shear stresses between the oxide scale and the MC spinel-coating layer are much higher as illustrated in Fig. 6. Fig. 8 shows the predicted shear stress contour at the critical indentation load of 90 kgf for the spinel-coated Crofer tri-layer system of sample 2. A very high interfacial shear stress is predicted at the spinel-coating/oxide scale interface. In addition, a localized region with very high shear stress is also predicted in the spinel coating right underneath the indenter contact radius. Therefore, in addition to the interfacial delamination, the indentation process may also cause localized spinel coating failure due to the highly concentrated shear stress predicted in the coating layer. The SEM cross-section of the indented tri-layer system in Fig. 7 confirms this prediction. When failure occurs first in the spinel coating, the subsequent interfacial failure at the spinel-coat/oxide scale interface can be considered as the result of crack propagation. The predicted interfacial stress at the spinel-coating and oxide-scale interface at the corresponding critical indentation loads can be considered as the lower bounds of the true interfacial strength at that interface.

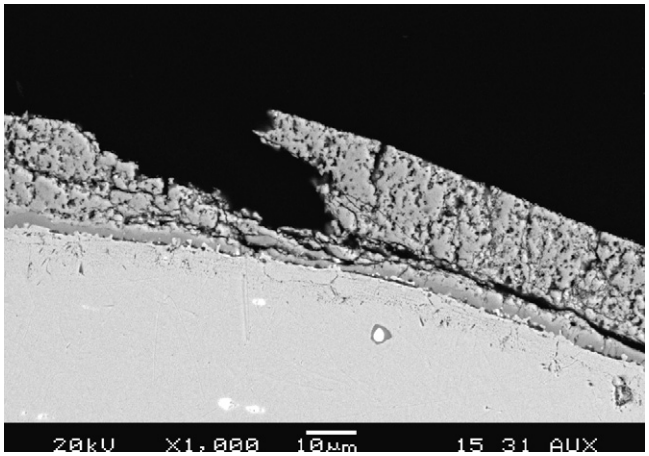

Fig. 7. SEM image of failed spinel-coated Crofer.

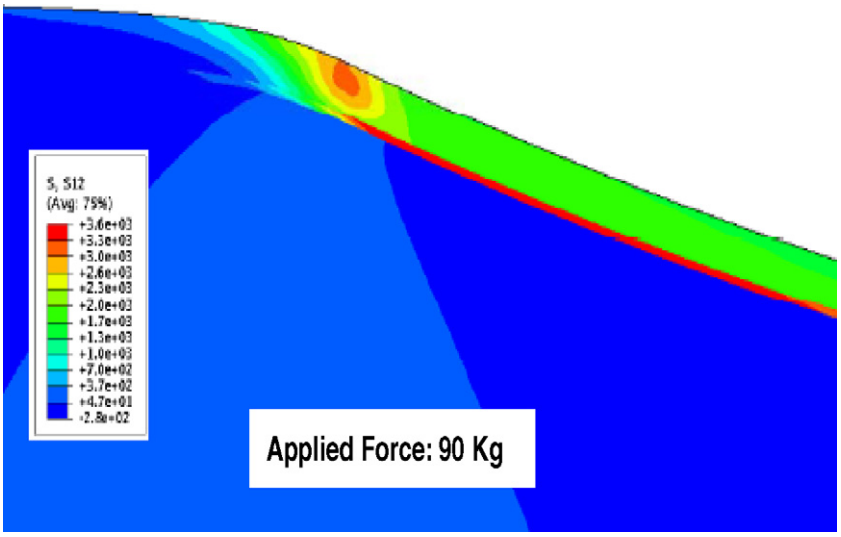

Fig. 8. Predicted shear stress distribution for oxidized, spinel-coated Crofer tri-layer system.

Results in Fig. 6 indicate that the lower bound of this interfacial strength is 886 MPa.

4. Life prediction of uncoated and coated metallic interconnect

The interfacial strengths quantified in the previous section for the two interfaces can now be used to determine the lifetime of a Crofer 22 APU with or without a spinel coating layer by comparing them with the interfacial stresses developed during SOFC stack cooling processes. Fig. 9 illustrates the flow chart of the life prediction methodology.

First, stack-cooling-induced interfacial shear stresses are calculated for a 0.5 mm thick Crofer 22 APU with different subscale thicknesses using FE analyses. The critical oxide scale thickness is determined by comparing the predicted interfacial shear stress with the interfacial strength quantified in the previous section. The corresponding oxidation time needed to form this critical oxide thickness can then be determined using the oxide-growth kinetics charts for Crofer 22 APU with and without a spinel coating layer. The oxidation time is therefore the IC lifetime predicted under stack cooling.

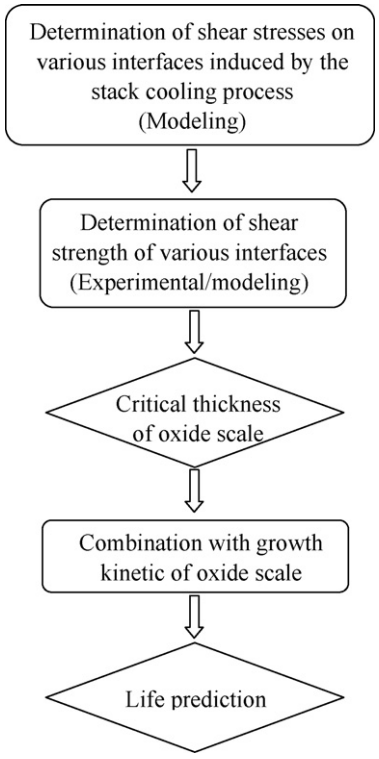

Fig. 9. Flow chart of life prediction of metallic interconnect in SOFC application.

4.1. Predictions of interfacial stresses during isothermal stack cooling

Because of the CTE mismatch between the oxide scale and the Crofer substrate, very high compressive stresses develop in the oxide scale during the stack cooling process [39]. In addition, interfacial shear stresses also develop at the edges of the IC plate [40]. The predicted interfacial shear stress increases with the growth of the oxide-scale thickness for an oxidized, uncoated Crofer 22 APU. Fig. 10 illustrates the evolution of cooling-induced interfacial shear stresses between the oxide scale and the Crofer substrate for various scale thicknesses, where the thermal and mechanical properties of the oxide scale and Crofer substrate are the same as given in the section of "Finite element model and material properties". In the

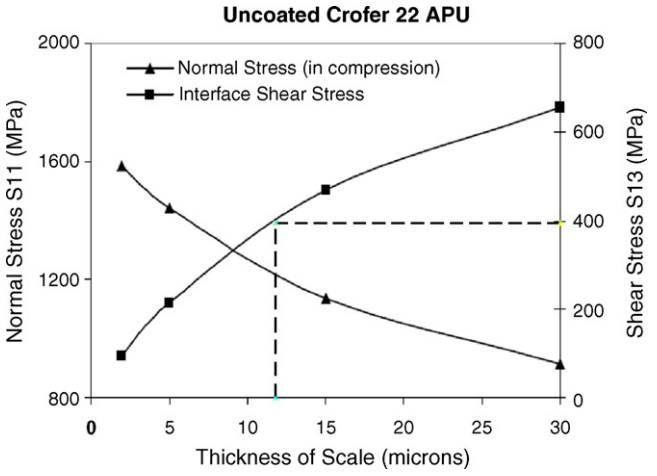

Fig. 10. Increase of predicted interfacial shear stress with growth of oxide scale under isothermal cooling conditions for uncoated Crofer 22 APU.

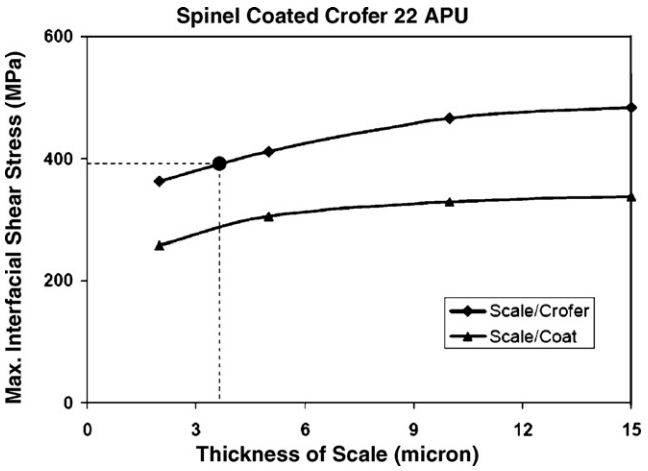

Fig. 11. Increase of interfacial shear stress with growth of oxide scale under isothermal cooling conditions for spinel-coated Crofer 22 APU.

following analysis of the oxidized, spinel-coated Crofer 22 APU, the same set of the thermal-mechanical properties is adapted, too.

For uncoated Crofer, the interfacial strength of the oxide scale and the Crofer substrate quantified in Fig. 5 can now be used in conjunction with Fig. 10 to quantify the critical oxide scale thickness at which interfacial fracture/delamination will occur during isothermal cooling. The critical oxide thickness is determined in Fig. 10 as 11.2 μm under isothermal cooling.

For spinel-coated Crofer 22 APU, assuming the thickness of the spinel coating is 15 μm, the maximum cooling-induced (from 800 °C to room temperature) interfacial shear stresses at the scale/substrate interface and the scale/spinel interface are calculated for various subscale thicknesses as shown in Fig. 11. At both interfaces, the cooling-induced maximum interfacial shear stresses increase with scale growth. It is also illustrated that the interfacial shear stresses on the oxide scale/Crofer interface are much higher than that on the oxide scale/spinel coating interface. Meanwhile, the quantified interfacial strength at the oxide scale/Crofer interface is much lower than that of the oxide scale/spinel coating interface. Therefore, cooling-induced spallation will occur at the oxide/Crofer interface. Assuming a constant interfacial strength of 395 MPa, the critical oxide scale thickness for interfacial fracture/delamination can be identified as 4.2 μm as shown in Fig. 11.

4.2. IC life determination with scale growth kinetics

After determination of the critical thickness of the oxide scale, the lifetime of Crofer 22 interconnect with or without coating may be estimated in conjunction with the oxide growth kinetics obtained experimentally under typical SOFC operating temperatures and environments.

For example, Fig. 12 depicts the experimentally determined oxide scale growth kinetics for bare and spinel-coated Crofer 22 APU under the typical SOFC operating condition of 800 °C [41]. The solid lines represent the growth kinetics curves of the oxide scale with and without coating with respect to oxidation time, i.e., working time in operating environments of SOFC, and the dashed lines represent the critical thickness of the oxide scale obtained in the previous section for uncoated and MC spinel-coated Crofer 22 APU. In Fig. 12, the light grey squares represent the measurement results of the oxide scale under the cycling thermal process with a 12-h span at 800 °C in air. The oxide scale for both uncoated and MC spinel-coated Crofer 22 APU grows linearly with respect to the square root of the oxidization time under the normal operating temperature of 800 °C.The oxide-growth kinetics for uncoated and MC

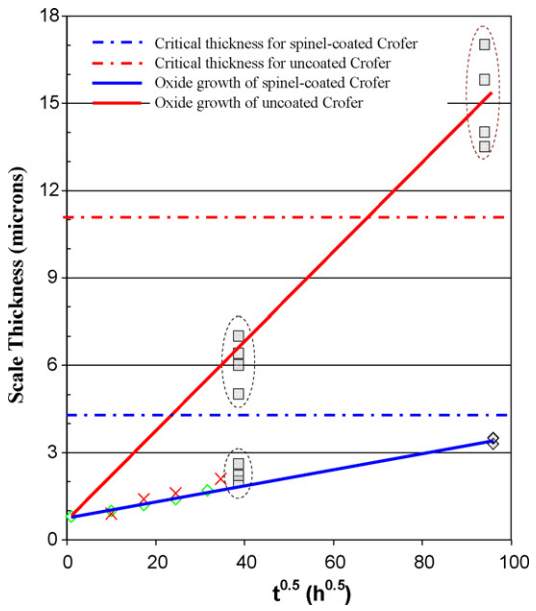

Fig. 12. Oxide scale growth kinetics for bare and spinel-coated Crofer 22 APU [41].

spinel-coated Crofer 22 APU shown in Fig. 12 can be approximated as

$$h = \begin{cases} 0.15455\,t^{1/2} + 0.751 & \text{for uncoated Crofer 22 APU} \\ 0.0277\,t^{1/2} + 0.751 & \text{for MC spinel-coated Crofer 22 APU} \end{cases},$$

where h is the oxide thickness in μm, and t is the time in h. Using the previously determined critical oxide thicknesses uncoated and spinel-coated Crofer 22 APU of

$$h_{cr} = \begin{cases} 11.4\,\mu m & \text{for uncoated Crofer 22 APU} \\ 4.2\,\mu m & \text{for MC spinel-coated Crofer 22 APU} \end{cases},$$

the lifetime for the uncoated and spinel-coated Crofer can be obtained, respectively as

$$t_L = \begin{cases} 4747\,h & \text{for uncoated Crofer 22 APU} \\ 15504\,h & \text{for MC spinel-coated Crofer 22 APU} \end{cases}$$

The predicted lifetime for the uncoated and MC spinel-coated Crofer are 4747 h and 15,504 h, respectively. As expected, a significantly longer lifetime is predicted for the coated Crofer than the uncoated one. Again, this shows the effectiveness of the spinel coating layer in delaying oxide growth and in prolonging the working lifetime of a Crofer 22 APU. It should be noted that the predicted lifetime of 15,504 h might still not be long enough for the designed lifetime of an SOFC stack. The coating thickness may need to be optimized to manage the subscale growth kinetics and therefore further improve the lifetime of Crofer 22 as an IC for planar SOFC applications.

5. Conclusions

In this paper, the integrated experimental/modeling approach is presented and applied to predict the lifetime of uncoated and coated metallic ICs used in SOFCs. The interfacial shear strengths of the oxide scale/Crofer 22 interface and the oxide scale/MC spinel coating interface were determined by indentation experiments and modeling. The critical oxide thickness for spallation is determined by comparing the interfacial strength with the cooling-induced interfacial stress for various oxide scale thickness. The critical oxide thickness is then used in conjunction with the experimentally determined oxide growth kinetics charts to predict the lifetime of

the coated and uncoated metallic ICs used in SOFC.Based on the results of our integrated experimental and analytical studies, we have reached the following conclusions:

(1) The MC spinel coating layer effectively prolongs the lifetime of the metallic interconnects used in SOFC. In the examples shown here, the predicted lifetime of the coated Crofer 22 APU is around 15,500 h, whereas the predicted lifetime of an uncoated Crofer 22 APU under the same environment is only around 4747 h.
(2) The cooling-induced interfacial stresses increase with the growth of the oxide scale.
(3) The interfacial strength between the oxide scale and the Crofer 22 substrate decreases with the growth of the oxide scale, indicating that the growth of the oxide scale will possibly degrade the IC interfacial reliability and therefore influence the long-term stack performance.
(4) The interfacial adhesion strength of the oxide scale/spinel-coating interface is much higher than that of the oxide scale/substrate interface.

It should be mentioned that the goal of this paper is to provide a methodology in predicting the life of metallic ICs. Since there is a generic variation in the critical indentation forces obtained through the indentation experiments, more specimens will be needed to obtain the actual critical indentation force. Our future work will also include applying similar methodology in identifying the effects of a surface finish on the interfacial strength between the native oxide layer and the metallic IC substrates. In addition, we will continue to investigate the degradation mechanisms of interfacial strength with oxide-scale growth.

Acknowledgements

The Pacific Northwest National Laboratory is operated by Battelle for the U.S. Department of Energy under Contract DE-AC05-76RL01830. The work was funded as part of the Solid-State Energy Conversion Alliance Core Technology Program by the U.S. Department of Energy's National Energy Technology Laboratory.

References

[1] J.W. Fergus, Materials Science & Engineering A (Structural Materials: Properties, Microstructure and Processing) 397 (1/2) (2005) 271–283.
[2] Z. Yang, G. Xia, J.W. Stevenson, Electrochemical and Solid-State Letters 8 (3) (2005) 168–170.
[3] Z. Yang, J.S. Hardy, M.S. Walker, G. Xia, S.P. Simner, J.W. Stevenson, Journal of the Electrochemical Society 151 (11) (2004) A1825–A1831.
[4] S. Chevalier, C. Valot, G. Bonnet, J.C. Colson, J.P. Larpin, Materials Science & Engineering A (Structural Materials: Properties, Microstructure and Processing) A343 (1/2) (2003) 257–264.
[5] A. Bautista, F. Velasco, J. Abenojar, Corrosion Science 45 (6) (2003) 1343–1354.
[6] W. Qu, J. Li, D.G. Ivey, Journal of Power Sources 138 (1/2) (2004) 162–173.
[7] I.M. Wolff, L.E. Iorio, T. Rumpf, P.V.T. Scheers, J.H. Potgieter, Materials Science & Engineering A (Structural Materials: Properties, Microstructure and Processing) A241 (1/2) (1998) 264–276.
[8] A. Martinez-Villafane, J.G. Chacon-Nava, C. Gaona-Tiburcio, F. Almeraya-Calderon, G. Dominguez-Patino, J.G. Gonzalez-Rodriguez, Materials Science & Engineering A (Structural Materials: Properties, Microstructure and Processing) A363 (1/2) (2003) 15–19.
[9] G.H. Meier, F.S. Pettit, Fundamental studies of the durability of materials for interconnects in solid oxide fuel cells (SOFCs), FY 2004 Annual Report, National Energy Technology Laboratory, U.S. Department of Energy, 2004.
[10] F.J. Perez, M.J. Cristobal, M.P. Hierro, F. Pedraza, G. Arnau, T.P. Merino, Surface and Coatings Technology 126 (2/3) (2000) 116–122.
[11] X. Yu, Y. Sun, Materials Science & Engineering A 363 (1/2) (2003) 30–39.
[12] A. Holt, P. Kofstad, Solid State Ionics, Diffusion & Reactions 117 (1/2) (1999) 21–25.
[13] B. Hua, J. Pu, W. Gong, J.F. Zhang, F.S. Lu, L. Jian, Journal of Power Sources 185 (1) (2008) 419.
[14] X. Chen, P.Y. Hou, C.P. Jacobson, S.J. Visco, L.C. De Jonghe, Solid State Ionics 176 (5/6) (2005) 425–433.
[15] Z.G. Yang, G.G. Xia, X.H. Li, J.W. Stevenson, International Journal of Hydrogen Energy 32 (16) (2007) 3648–3654.
[16] M.J. Garcia-Vargas, M. Zahid, F. Tietz, A. Aslanides, ECS Transactions 7 (1 (Part 2)) (2007) 2399–2405.
[17] D.G. Ivey, W. Qu, J. Li, J.M. Hill, Journal of Power Sources 153 (1) (2006) 114–124.
[18] M. Bertoldi, T. Zandonella, D. Montinaro, V.M. Sglavo, A. Fossati, A. Lavacchi, C. Giolli, U. Bardi, Journal of Fuel Cell Science and Technology 5 (1) (2008) 011001-1–011001-5.
[19] M. Schulte, M. Schutze, Oxidation of Metals 51 (1/2) (1999) 55–77.
[20] S.R. Pillai, N.S. Barasi, H.S. Khatak, J.B. Gnanamoorthy, Oxidation of Metals 49 (5/6) (1998) 509–530.
[21] V.K. Tolpygo, J.R. Dryden, D.R. Clarke, Acta Materialia 46 (3) (1998) 927–937.
[22] W. Przybilla, M. Schutze, Oxidation of Metals 58 (3/4) (2002) 337–359.
[23] J. Mougin, A. Galerie, M. Dupeux, N. Rosman, G. Lucazeau, A.M. Huntz, L. Antoni, Materials and Corrosion 53 (7) (2002) 486–490.
[24] X. Sun, W.N. Liu, P. Singh, M.A. Khaleel, Effects of Oxide Thickness on Scale and Interface Stresses under Isothermal Cooling and Micro-Indentation, PNNL-15794, Pacific Northwest National Laboratory, Richland, WA, 2006.
[25] Y.M. Xu, H.M. Wang, Journal of Alloys and Compounds 457 (1/2) (2008) 239–243.
[26] P.Y. Hou, A.P. Paulikas, B.W. Veal, J.L. Smialek, Acta Materialia 55 (16) (2007) 5601–5613.
[27] J.Y. Kim, V.L. Sprenkle, N.L. Canfield, K.D. Meinhardt, L.A. Chick, Journal of the Electrochemical Society 153 (5) (2006) A880–A886.
[28] A. Vasinonta, J.L. Beuth, Engineering Fracture Mechanics 68 (2001) 843–860.
[29] M.D. Drory, J.W. Hutchinson, Proceedings of the Materials Research Society, vol. 383, 1995, pp. 173–182.
[30] X. Sun, W. Liu, E.V. Stephens, M.A. Khaleel, Journal of Power Sources 176 (2008) 167–174.
[31] ABAQUS/Standard User's Manual, Hibbitt, Karlsson and Sorensen Inc., 2002.
[32] A.M. Huntz, Materials Science & Engineering A201 (1995) 211–228.
[33] J.J. Barnes, J.G. Goedjen, D.A. Shores, Oxidation of Metals 32 (5/6) (1989) 449–469.
[34] M. Chou, G. Xia, PNNL Internal Communication (2007).
[35] Material Data Sheet No. 4046: Crofer 22 APU, ThyssenKrupp VDM, Werdohl, Germany, 2005.
[36] R. Hojda1, L. Paul, Proceedings of Materials Science & Technology, 2005, pp. 155–163.
[37] Young's Modulus of Crofer 22 APU, ThyssenKrupp VDM, Werdohl, Germany, 2006.
[38] S. Chandra-Ambhorn, Y. Wouters, L. Antoni, F. Toscan, A. Galerie, Journal of Power Sources 171 (2007) 688–695.
[39] G. Calvarin, A.M. Huntz, A. Hugot Le Goff, S. Joiret, M.C. Bernard, Scripta Materialia 38 (11) (1998) 1649–1658.
[40] X. Sun, W.N. Liu, P. Singh, M.A. Khaleel, Effects of oxide thickness on scale and interface stresses under isothermal cooling and micro-indentation, Technical Report, PNNL-15794, Pacific Northwest National Laboratory, Richland, WA, 2006.
[41] J.W. Stevenson, Z.G. Yang, G.G. Xia, G.D. Maupin, X.S. Li, P. Singh, 7th Annual SECA Workshop and Peer Review, Philadelphia, PA, 2006.